Journal of Solid State Chemistry 181 (2008) 2393–2400

Contents lists available at ScienceDirect

Journal of Solid State Chemistry

journal homepage: www.elsevier.com/locate/jssc

Phase relations in the $K_2W_2O_7$–K_2WO_4–KPO_3–Bi_2O_3 system and structure of $K_{6.5}Bi_{2.5}W_4P_6O_{34}$

K.V. Terebilenko [a], I.V. Zatovsky [a,*], V.N. Baumer [b], I.V. Ogorodnyk [a], N.S. Slobodyanik [a], O.V. Shishkin [b]

[a] Inorganic Chemistry Department, Kiev University, Volodimirska Street 64, Kiev 01033, Ukraine
[b] STC "Institute for Single Crystals" NAS of Ukraine, 60 Lenin ave., Kharkiv 61001, Ukraine

ARTICLE INFO

Article history:
Received 31 January 2008
Received in revised form
19 May 2008
Accepted 25 May 2008
Available online 3 July 2008

Keywords:
Composition diagram
Flux
Bond valence sum
Tungstate
Phosphate

ABSTRACT

The phase relations in the cross-section of the $K_2W_2O_7$–K_2WO_4–KPO_3 containing 15 mol% Bi_2O_3 were undertaken using flux method. Crystallization fields of $K_{6.5}Bi_{2.5}W_4P_6O_{34}$, $K_2Bi(PO_4)(WO_4)$, Bi_2WO_6, $KBi(WO_4)_2$ and their cocrystallization areas were identified. Novel phase $K_{6.5}Bi_{2.5}W_4P_6O_{34}$ was characterized by single-crystal X-ray diffraction: sp. gr. $P-1$, $a = 9.4170(5)$, $b = 9.7166(4)$, $c = 17.6050(7)$ Å, $\alpha = 90.052(5)^\circ$, $\beta = 103.880(5)^\circ$ and $\gamma = 90.125(5)^\circ$. It has a layered structure, which contains $\{K_7Bi_5W_8P_{12}O_{68}\}_\infty$ layers stacked parallel to *ab* plane and sheets composed by potassium atoms separating these layers. Sandwich-like $\{K_7Bi_5W_8P_{12}O_{68}\}_\infty$ layers are assembled from $[W_2P_2O_{13}]_\infty$ and $[BiPO_4]_\infty$ building units, and are penetrated by tunnels with K/Bi atoms inside. FTIR-spectra of $K_2Bi(PO_4)(WO_4)$ and $K_{6.5}Bi_{2.5}W_4P_6O_{34}$ were discussed on the basis of factor group theory.

1. Introduction

Flux growth method is widely used for preparation single crystals of phosphates, molybdates and tungstates. Complex phosphate–molybdate or phosphate–tungstate fluxes are suitable for crystal growth experiments where desired crystalline compounds can be obtained. In this aspect, these multicomponent systems offer a perfect combination of melting point, vapor pressure and ability to grow different types of compounds [1–4].

From synthetic point of view, there are two main applications of mixed phosphate–tungstate melts. Firstly, molten alkaline tungstates or tungsten (VI) oxide provide a good reaction medium for the crystal growth of phosphates. For instance, $AgV_2(PO_4)(P_2O_7)$ [5] and $KTiOPO_4$ [6,7] were yielded from WO_3-containing solutions. On the other hand, under mentioned conditions tungstate-containing phosphates $K_2M^{II}WO_2(PO_4)_2$ (M^{II} = Ni, Mg) [8,9] with W(VI) in octahedral coordination were easily prepared in K_2WO_4–WO_3 and KPO_3 fluxes. Up to date, there are only two examples of the coexistence of both WO_4 and PO_4 tetrahedra in one compound: $Zr_2(WO_4)(PO_4)_2$ [10] and $K_2Bi(PO_4)(WO_4)$ [11].

Complex investigations of phosphate–tungstate systems containing mono- and polyvalent metal oxides may reveal possibilities of successful crystal growth of huge diversity of compounds with phosphate, tungstate or mixed sublattice and define the relationship, which exists between the initial composition in charge and composition of final phase.

Bismuth-containing compounds were suggested as promising materials with useful properties: ionic conductivity [12,13], superplasticity [14], nonlinear optic properties and photoluminescence [15,16]. The section of $K_2W_2O_7$–K_2WO_4–KPO_3 containing 15 mol% Bi_2O_3 was selected as the most favorable for crystal growth during our prior investigations in the K–Bi–P–W–O system [11].

Herein, phase relations in $K_2W_2O_7$–K_2WO_4–KPO_3–Bi_2O_3 pseudo-quaternary system, crystal structure of $K_{6.5}Bi_{2.5}W_4P_6O_{34}$, IR-spectra and thermal behavior of obtained compounds are presented.

2. Experimental

2.1. Study of phase formation

Crystallization fields of compounds in the $K_2W_2O_7$–K_2WO_4–KPO_3–Bi_2O_3 system were defined on the basis of phase analyses of flux growth products. Detailed investigation was performed in molten system containing variable contents of $K_2W_2O_7$, K_2WO_4 and KPO_3 (solvent) at constant molar content of Bi_2O_3 (15%). The latter amount was calculated with respect to the point $xK_2W_2O_7$–yK_2WO_4–$zKPO_3$ chosen on ternary diagram (Fig. 1) to result a final four-component mixture with composition $0.85xK_2W_2O_7$–$0.85yK_2WO_4$–$0.85zKPO_3$–$0.15Bi_2O_3$.

* Corresponding author.
E-mail address: Zvigo@yandex.ru (I.V. Zatovsky).

0022-4596/$ - see front matter © 2008 Elsevier Inc. All rights reserved.
doi:10.1016/j.jssc.2008.05.035

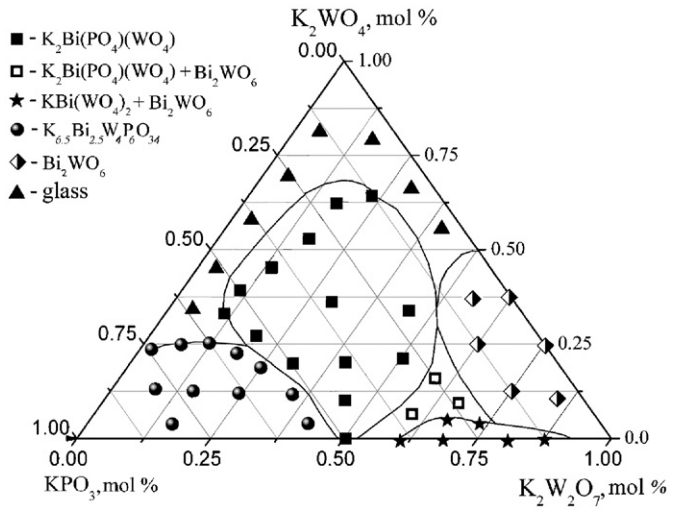

Fig. 1. Composition diagram of $K_2W_2O_7$–K_2WO_4–KPO_3 system containing 15 mol% Bi_2O_3 with approximate fields of crystallization.

The reagents K_2CO_3, WO_3, KPO_3 and Bi_2O_3 used were of analytical grade purity. K_2WO_4 and $K_2W_2O_7$ were prepared from the mixtures of K_2CO_3 and WO_3 in appropriate ratio 1:1 and 1:2 by slow heating to 1223 K and annealing for 1 h.

The methodology of the high-temperature investigations was as follows. The charges prepared from the calculated amounts of $K_2W_2O_7$, K_2WO_4, KPO_3 and Bi_2O_3 were well ground and melted in platinum crucibles at 1200 K for 2 h to reach homogeneity. After that, transparent solutions were cooled to 750–850 K at a rate 30–10 K/h and, finally, quenched to room temperature. It should be admitted that in several cases nucleation and crystallization in the fluxes were initiated by intensive stirring with platinum stirrer. The solidified melt was leached out with hot water to recover obtained crystals. Phase identification was performed using powder X-ray diffraction (XRD) and optical microscopy.

2.2. Synthesis of $K_{6.5}Bi_{2.5}W_4P_6O_{34}$

Investigation of phase formation in the system has revealed a special feature of $K_{6.5}Bi_{2.5}W_4P_6O_{34}$ to crystallize in scratched and crashed form. More detailed study was performed to determine appropriate growth window and to obtain suitable crystals for structure investigations. As a result, it was grown successfully according to the following pathway. A mixture of 8.39 g $K_2W_2O_7$, 3.61 g K_2WO_4, 10.74 g KPO_3 and 9.75 g Bi_2O_3 was homogenized at 1200 K for 2 h and cooled down to 750 K at a rate 10 K/h. Stirring of the melt was necessary to activate the crystallization during slow cooling. Colorless prismatic crystals were selected from remaining flux after quenching to room temperature and washing out with hot water (72% yield by Bi).

The inductively coupled plasma-atomic emission spectroscopy (ICP-AES) determination of the potassium, phosphorus, tungsten and bismuth amounts in prepared crystals was performed on a "Spectroflame Modula ICP" ("Spectro", Germany) instrument. Elemental analysis calculated (%) for $K_{6.5}Bi_{2.5}W_4P_6O_{34}$ (1096.91): K 11.58, Bi 23.81, W 33.52, P 8.47; found K 11.63, Bi 23.79, W 33.41, P 8.53.

2.3. XRD

The structures of $K_{6.5}Bi_{2.5}W_4P_6O_{34}$ and $KBi(WO_4)_2$ were determined from single-crystal XRD data. Prismatic crystals of $KBi(WO_4)_2$ were selected from the mixture of $KBi(WO_4)_2$+Bi_2WO_6, grown in the cocrystallization point. Single-crystal diffraction experiments were performed using an Oxford Diffraction XCalibur-3 diffractometer equipped with 4 Mpixel CCD detector.

The structures were solved using direct methods with SHELXS-97 [17] and refined using full-matrix least-squares technique in anisotropic approximation with SHELXL-97 [18]. Structure solution and refinement of $KBi(WO_4)_2$ was performed in a routine manner, while the refinement of $K_{6.5}Bi_{2.5}W_4P_6O_{34}$ was accompanied by specific operations. The heavy atoms were located by structure solution, whereas the remaining oxygen atoms were found using Fourier maps calculated during refinement. Similar environment of potassium, bismuth atoms and distortions of their polyhedra lead to difficulties of interpretation of atom type. Finally, it was suggested that several positions could be occupied by both potassium and bismuth. The occupancies of corresponding atoms were refined using free variables. The extinction correction was applied, but as its value was found negligible comparing with its deviation, it was removed from the final cycles of the refinement. In case of the refinement when the positions (K5/Bi5, K6/Bi6, K7/Bi7, K8/Bi8) occupied by only one kind of atom (K or Bi) the agreement factors (R, w*R*, Goof) were higher than in the described above refinement with partial occupation and their ADP were found to be unreasonable. Thus, these positions were suggested to be occupied by both K and Bi. The coordinates and ADP of corresponding atoms (example K5 and Bi5) were

Table 1
Crystallographic data and structure refinement of $K_{6.5}Bi_{2.5}W_4P_6O_{34}$

	$K_{6.5}Bi_{2.5}W_4P_6O_{34}$
Crystal data	
Crystal system	Triclinic
Space group	*P*-1 (no. 2)
Cell parameter (Å)	
a	9.4170(5)
b	9.7166(4)
c	17.6050(7)
α (deg)	90.052(5)
β (deg)	103.880(5)
γ (deg)	90.125(5)
V (Å^3)	1563.84(12)
Z	2
$\rho_{calc.}$ (g/cm^3)	4.761
Crystal dimensions (mm)	0.1 × 0.08 × 0.04
Data collection	
Diffractometer	XCalibur 3 CCD
Mo*K*α radiation (Å)	0.71073
Monochromator	Graphite
Scan mode	φ and ω
μ (mm^{-1})	29.96
Absorption correction	Multi-scan
Meas. temperature (K)	293(2)
T_{min}, T_{max}	0.102, 0.380
Number of reflections	17393
Independent reflections	9098
Reflections with $I>2\sigma(I)$	8355
$R_{int.}$	0.049
Theta range (deg)	2.77–30.06
$h=, k=, l=$	−13→13; −13→13; −24→24
F(000)	1978
Solution and refinement	
Primary solution method	Direct
Weighting scheme	$w=1/[\sigma^2(Fo^2)+(0.054P)^2+23.3102P]$, where $P=(Fo^2+2Fc^2)/3$
$R_1[F^2>2\sigma(F^2)]$	0.035
R_1(all)	0.041
wR_2	0.097
S	1.103
Number of parameters	491
Extinction correction	None
$(\Delta\rho)_{max,\ min}$ (e/Å^3)	2.956, −2.194

constrained. The charge of the definitely located atoms was calculated. The remaining positive charge of the partially occupied atoms was used as the restrained value in the occupancies refinement. The charge of K and Bi atoms was restrained (SUMP restraints) by noted above value and the refinement was performed. As it was found, the composition obtained during the refinement is close to those found by element analysis.

Crystal data and refinement for $K_{6.5}Bi_{2.5}W_4P_6O_{34}$ is listed in Table 1 as well as the coordinates and U_{eq} of the atoms in Table 2. Selected geometric parameters and bond valence sum (BVS) for $K_{6.5}Bi_{2.5}W_4P_6O_{34}$ are gathered in Table 3. Further details of the crystal structure investigations can be obtained from the Fachinformationszentrum Karlsruhe, 76344 Eggenstein-Leopoldshafen, Germany (fax: +49 7247 808 666; e-mail: crysdata@fiz-karlsruhe.de) on quoting the depository number CSD-419115 for $K_{6.5}Bi_{2.5}W_4P_6O_{34}$ and CSD-419114 for $KBi(WO_4)_2$.

Powder pattern of $K_{6.5}Bi_{2.5}W_4P_6O_{34}$ was collected using a Siemens D500 diffractometer (Cu$K\alpha$ radiation, $\lambda = 1.54184$ Å; curved graphite monochromator on the counter arm; $2^\circ \leqslant 2\theta \leqslant 100^\circ$, scan step 0.02°, dwell time 40 s) to identify cell dimensions: $a = 9.4225(4)$ Å, $b = 9.7114(4)$ Å, $c = 17.5990(6)$ Å, $\alpha = 90.012(3)^\circ$, $\beta = 103.895(3)^\circ$, $\gamma = 90.617(3)^\circ$, $V = 1563.19(10)$ Å^3.

Table 2
The coordinates and equivalent isotropic thermal parameters of the atoms for $K_{6.5}Bi_{2.5}W_4P_6O_{34}$

Atom	Site	Occ. (<1)	*x*	*y*	*z*	U_{eq}
W_1	2*i*		0.93561 (5)	−0.13186 (5)	0.66523 (3)	0.01091 (9)
W_2	2*i*		0.20519 (5)	0.13355 (5)	0.63733 (3)	0.01069 (9)
W_3	2*i*		0.41733 (5)	0.63175 (5)	0.64302 (3)	0.01109 (9)
W_4	2*i*		0.70899 (5)	0.37457 (5)	0.64782 (3)	0.01106 (9)
Bi_1	2*i*		0.85272 (5)	0.37381 (6)	0.88911 (3)	0.01457 (9)
Bi_2	2*i*		0.68234 (5)	0.84733 (5)	1.10771 (3)	0.01409 (10)
K_1	1*f*		0.5	0	0.5	0.0242 (9)
K_2	2*i*		0.8377 (4)	0.1624 (4)	0.5022 (2)	0.0340 (8)
K_3	2*i*		0.6661 (4)	−0.3328 (4)	0.5045 (2)	0.0270 (7)
K_4	1*g*		0	0.5	0.5	0.0211 (9)
K_5	2*i*	0.956(3)	0.6099 (4)	0.0111 (4)	0.7138 (2)	0.0409 (10)
Bi_5	2*i*	0.044(3)	0.6099 (4)	0.0111 (4)	0.7138 (2)	0.0409 (10)
K_6	2*i*	0.9443(17)	0.1041 (4)	0.5126 (4)	0.7242 (2)	0.0406 (9)
Bi_6	2*i*	0.056	0.1041 (4)	0.5126 (4)	0.7242 (2)	0.0406 (9)
K_7	2*i*	0.925 (3)	0.4945 (5)	0.6052 (5)	0.8999 (2)	0.0675 (14)
Bi_7	2*i*	0.075 (3)	0.4945 (5)	0.6052 (5)	0.8999 (2)	0.0675 (14)
K_8	2*i*	0.675 (3)	1.0066 (11)	−0.1773(11)	0.9068 (4)	0.302 (6)
Bi_8	2*i*	0.325 (3)	1.0066 (11)	−0.1773(11)	0.9068 (4)	0.302 (6)
P_1	2*i*		0.1772 (4)	0.4315 (4)	0.95817 (19)	0.0133 (6)
P_2	2*i*		0.4605 (3)	0.3477 (3)	0.75384 (17)	0.0122 (6)
P_3	2*i*		0.7567 (4)	−0.3371 (3)	0.76187 (19)	0.0110 (6)
P_4	2*i*		1.3267 (4)	−0.0748 (4)	1.05025 (18)	0.0117 (6)
P_5	2*i*		0.2903 (3)	−0.1370(4)	0.75897 (17)	0.0116 (5)
P_6	2*i*		0.9824 (4)	0.1755 (3)	0.76004 (18)	0.0109 (6)
O_1	2*i*		0.4175 (13)	0.4982 (11)	0.7401 (6)	0.023 (2)
O_2	2*i*		0.3167 (12)	0.7455 (11)	0.7047 (8)	0.027 (3)
O_3	2*i*		0.1217 (15)	0.4920 (14)	0.8773 (6)	0.035 (3)
O_4	2*i*		0.5455 (10)	0.4942 (10)	0.6161 (5)	0.0150 (19)
O_5	2*i*		0.3854 (12)	0.8485 (12)	0.8392 (6)	0.028 (2)
O_6	2*i*		0.7767 (11)	0.6362 (10)	0.8479 (5)	0.0204 (19)
O_7	2*i*		0.8589 (11)	−0.2178 (11)	0.7520 (6)	0.019 (2)
O_8	2*i*		1.0494 (11)	0.3616 (12)	0.9847 (5)	0.023 (2)
O_9	2*i*		0.5999 (10)	−0.2879 (10)	0.7225 (5)	0.0139 (19)
O_{10}	2*i*		0.6977 (11)	0.6727 (10)	1.0385 (6)	0.021 (2)
O_{11}	2*i*		0.3661 (12)	0.2575 (12)	0.6869 (6)	0.024 (2)
O_{12}	2*i*		0.4454 (11)	0.3077 (10)	0.8350 (5)	0.018 (2)
O_{13}	2*i*		0.8048 (12)	0.4287 (12)	0.5787 (6)	0.022 (2)
O_{14}	2*i*		0.7485 (10)	0.4553 (11)	0.9800 (6)	0.019 (2)
O_{15}	2*i*		0.6231 (13)	−0.0072 (14)	0.8722 (7)	0.031 (3)
O_{16}	2*i*		0.3259 (12)	−0.0013 (10)	0.7247 (7)	0.023 (2)
O_{17}	2*i*		0.2546 (11)	0.5530 (10)	0.5913 (6)	0.022 (2)
O_{18}	2*i*		1.0524 (11)	−0.0030 (10)	0.6201 (5)	0.017 (2)
O_{19}	2*i*		0.4638 (10)	0.8654 (13)	1.0328 (6)	0.023 (2)
O_{20}	2*i*		0.7661 (9)	−0.0954 (10)	0.6048 (5)	0.0154 (19)
O_{21}	2*i*		0.6213 (10)	0.3297 (10)	0.7493 (5)	0.0156 (18)
O_{22}	2*i*		0.3041 (12)	0.0686 (12)	0.5737 (7)	0.029 (3)
O_{23}	2*i*		−0.1981 (12)	0.5431 (10)	0.7189 (6)	0.019 (2)
O_{24}	2*i*		0.1293 (9)	0.8547 (12)	0.7605 (5)	0.021 (2)
O_{25}	2*i*		0.7843 (11)	0.1814 (11)	0.9366 (7)	0.023 (2)
O_{26}	2*i*		0.7510 (10)	0.9831 (11)	1.0164 (6)	0.017 (2)
O_{27}	2*i*		0.9066 (12)	0.0425 (12)	0.7325 (6)	0.022 (2)
O_{28}	2*i*		−0.0230 (12)	0.7198 (10)	0.6215 (7)	0.024 (2)
O_{29}	2*i*		0.1277 (11)	0.1956 (11)	0.7349 (5)	0.016 (2)
O_{30}	2*i*		1.0106 (14)	0.1903 (13)	0.8454 (6)	0.031 (3)
O_{31}	2*i*		−0.1167 (11)	0.2919 (11)	0.7198 (7)	0.023 (2)
O_{32}	2*i*		0.1006 (12)	0.2601 (11)	0.5783 (6)	0.024 (2)
O_{33}	2*i*		0.4415 (14)	−0.2456 (12)	0.5762 (6)	0.029 (3)
O_{34}	2*i*		0.6304 (12)	0.2184 (10)	0.6060 (6)	0.022 (2)

Table 3
The bond lengths (Å) in the coordination polyhedra and BVS for $K_{6.5}Bi_{2.5}W_4P_6O_{34}$

								BVS	
WO_6 polyhedra									
W(1)–O(28)^{i}	1.722(10)	W(1)–O(20)	1.730(8)	W(1)–O(18)	1.955(9)			W(1)O_6	6.10
W(1)–O(7)	2.020(10)	W(1)–O(27)	2.122(11)	W(1)–O(24)^{i}	2.166(9)				
W(2)–O(22)	1.739(11)	W(2)–O(32)	1.755(11)	W(2)–O(18)^{iii}	1.925(10)			W(2)O_6	6.17
W(2)–O(11)	1.966(11)	W(2)–O(29)	2.110 (9)	W(2)–O(16)	2.132(10)				
W(3)–O(33)^{v}	1.727(10)	W(3)–O(17)	1.757(10)	W(3)–O(4)	1.936(10)			W(3)O_6	6.25
W(3)–O(2)	1.948(10)	W(3)–O(9)^{v}	2.088(9)	W(3)–O(1)	2.146(10)				
W(4)–O(13)	1.761(10)	W(4)–O(34)	1.768(10)	W(4)–O(4)	1.905(10)			W(4)O_6	5.95
W(4)–O(31)^{vii}	1.989(10)	W(4)–O(23)^{vii}	2.115(9)	W(4)–O(2)1	2.184(9)				
PO_4 tetrahedra									
P(1)–O(3)	1.514(11)	P(1)–O(10)^{ix}	1.545(10)	P(1)–(O8)^{iii}	1.547(11)	P(1)–O(14)^{ix}	1.585(10)	P(1)O_4	4.83
P(2)–O(12)	1.520(9)	P(2)–O(1)	1.522(11)	P(2)–O(21)	1.546(10)	P2–O(11)	1.561(11)	P(2)O_4	4.97
P(3)–O(6)^{x}	1.503(9)	P(3)–O(23)^{i}	1.505(10)	P(3)–O(7)	1.542(10)	P(3)–O(9)	1.550 (10)	P(3)O_4	5.14
P(4)–O(19)^{i}	1.515(10)	P(4)–O(26)^{xiii}	1.516(9)	P(4)–O(25)^{viii}	1.527(11)	P(4)–O(15)^{viii}	1.552(12)	P(4)O_4	5.10
P(5)–O(5)^{x}	1.486(10)	P(5)–O(16)	1.521(10)	P(5)–O(24)^{x}	1.525(9)	P(5)–O(2)^{x}	1.546(11)	P(5)O_4	5.21
P(6)–O(30)	1.468(11)	P(6)–O(27)	1.498(12)	P(6)–O(31)^{vii}	1.529(11)	P(6)–O(29)^{vii}	1.548(10)	P(6)O_4	5.35
BiO_X polyhedra									
Bi(1)–O(8)	2.187(10)	Bi(1)–O(25)	2.206(11)	Bi(1)–O(14)	2.216(10)	Bi(1)–O(30)	2.557(13)	Bi(1)O_8	3.02
Bi(1)–O(6)	2.702(10)	Bi(1)–O(3)^{vii}	2.832(15)	Bi(1)–O(21)	2.900(12)	Bi(1)–O(31)^{vii}	3.164(13)		
Bi(2)–O(10)	2.113(9)	Bi(2)–O(19)	2.169(9)	Bi(2)–O(26)	2.289(9)	Bi(2)–O(12)^{ix}	2.305(9)	Bi(2)O_7	3.21
Bi(2)–O(30)^{xiii}	2.835(13)	Bi(2)–O(29)^{ix}	2.946(12)	Bi(2)–O(5)^{ix}	3.210(13)				
K/BiO_X polyhedra									
K/Bi(5)–O(16)	2.730(12)	K/Bi(5)–O(27)	2.750(12)	K/Bi(5)–O(15)	2.766(12)	K/Bi(5)–O(34)	2.807(12)	K(5)O_{10}	1.04 (0.99)
K/Bi(5)–O(20)	2.877(10)	K/Bi(5)–O(9)	2.913(10)	K/Bi(5)–O(21)	3.153(11)	K/Bi(5)–O(7)	3.188(12)	Bi(5)O_{10}	1.07 (0.05)
K/Bi(5)–O(11)	3.276(12)	K/Bi(5)–O(22)	3.360(13)						
K/Bi(6)–O(3)	2.668(11)	K/Bi(6)–O(28)	2.781(12)	K/Bi(6)–O(23)	2.841(11)	K/Bi(6)–O(1)	2.900(12)	K(6)O_{10}	0.96 (0.91)
K/Bi(6)–O(31)	2.972(12)	K/Bi(6)–O(17)	3.038(11)	K/Bi(6)–O(29)	3.091(11)	K/Bi(6)–O(2)	3.092(13)	Bi(6)O_{10}	0.98 (0.05)
K/Bi(6)–O(24)	3.381(12)	K/Bi(6)–O(13)^{iii}	3.420(12)						
K/Bi(7)–O(5)	2.697(12)	K/Bi(7)–O(10)	2.793(11)	K/Bi(7)–O(14)	2.869(11)	K/Bi(7)–O(1)	2.921(11)	K(7)O_6	0.70 (0.65)
K/Bi(7)–O(6)	3.025(11)	K/Bi(7)–O(12)	3.100(11)					Bi(7)O_6	0.72 (0.05)
K/Bi(8)–O(8)^{viii}	2.761(12)	K/Bi(8)–O(7)	2.774(12)	K/Bi(8)–O(6)^{x}	2.820(12)	K/Bi(8)–O(25)^{viii}	2.979(12)	K(8)O_6	0.69 (0.46)
K/Bi(8)–O(26)^{xiii}	3.016(13)	K/Bi(8)–O(24)^{i}	3.080(12)					Bi(8)O_6	0.71 (0.23)
KO_X polyhedra									
K(1)–O(22)	2.585(11) × 2	K(1)–O(33)	2.856(11) × 2	K(1)–O(20)	2.888(8) × 2	K(1)–O(34)	2.894(10) × 2	K(1)O_8	1.16
K(2)–O(32)^{vii}	2.688(11)	K(2)–O(22)^{iv}	2.780(11)	K(2)–O(33)^{iv}	2.783(12)	K(2)–O(13)	2.967(11)	K(2)O_{10}	0.97
K(2)–O(18)	2.998(10)	K(2)–O(34)	3.027(11)	K(2)–O(18)^{ii}	3.029(10)	K(2)–O(17)^{vi}	3.231(11)		
K(2)–O(20)	3.253(11)	K(2)–O(28)^{vi}	3.304(11)						
K(3)–O(13)^{x}	2.826(12)	K(3)–O(33)	2.841(12)	K(3)–O(20)	2.917(10)	K(3)–O(17)^{iv}	2.930(11)	K(3)O_{11}	0.98
K(3)–O(22)^{iv}	2.958(13)	K(3)–O(4)^{iv}	2.981(10)	K(3)–O(32)^{iv}	2.997(12)	K(3)–O(4)^{x}	3.007(10)		
K(3)–O(28)^{i}	3.190(12)	K(3)–O(34)^{iv}	3.198(12)	K(3)–O(11)^{iv}	3.391(11)				
K(4)–O(17)	2.596(10) × 2	K(4)–O(13)^{iii}	2.644(10) × 2	K(4)–O(32)	2.760(11) × 2	K(4)–O(28)	3.066(11) × 2	K(4)O_8	1.31
K–K and Bi–K contacts									
K(1)–K(2)	3.539(4)	K(3)–K(4)^{i}	3.560(4)	K(1)–K(3)	3.587(4)	K(2)–K(4)^{vii}	3.620(4)		
Bi(1)–K(8)^{viii}	4.007(7)	K(7)–K(7)^{ix}	4.057(10)	Bi(1)–K(7)	4.100(5)	Bi(2)–K(7)	4.349(4)		
K(6)^{i}–K(8)	4.655(12)	K(8)–K(8)^{viii}	4.78(2)						

Symmetry transformations used to generate equivalent atoms: (i) $x+1, y-1, z$; (ii) $-x+2, -y, -z+1$; (iii) $x-1, y, z$; (iv) $-x+1, -y, -z+1$; (v) $x, y+1, z$; (vi) $-x+1, -y+1, -z+1$; (vii) $x+1, y, z$; (viii) $-x+2, -y, -z+2$; (ix) $-x+1, -y+1, -z+2$; (x) $x, y-1, z$; (xi) $-x, -y+1, -z+1$; (xii) $x-1, y+1, z$; (xiii) $-x+2, -y+1, -z+2$.

Qualitative and quantitative phase analyses of the grown products were carried out with a DRON-3 diffractometer (Cu$K\alpha$ radiation, $\lambda = 1.54184$ Å; Ni β-filter; $10^\circ \leqslant 2\theta \leqslant 60^\circ$, scan step 0.02°). Structural data of $K_2Bi(PO_4)(WO_4)$ [11], $KBi(WO_4)_2$ [19] and Bi_2WO_6 [20] were used for identification of known compounds.

2.4. Differential thermal analyses and IR-spectroscopy

Differential thermal analysis (DTA) was carried out on a Quasy-1500 thermal analyzer in the temperature range 293–1273 K (heating rate 5 K/min). The experiments were performed for a ground powder of selected single crystals of $K_2Bi(PO_4)(WO_4)$ and $K_{6.5}Bi_{2.5}W_4P_6O_{34}$, respectively.

The FTIR-spectra were studied in the range 400–1500 cm^{-1} and were collected at a room temperature in KBr disks using a NICOLET Nexus 470 (FTIR) spectrometer.

3. Results and discussion

3.1. Phase formation in the $K_2W_2O_7$–K_2WO_4–KPO_3–Bi_2O_3 system

The experimentally determined fields of phase crystallization in the investigated system are shown in Fig. 1. This diagram represents only approximate boundaries of different compounds but schematically gives enough quantitative information to grow desired compound and trace out general crystallization trends in the solution system.

Three regions of pure compounds and two biphasic fields were identified. Crystallization of new $K_{6.5}Bi_{2.5}W_4P_6O_{34}$ is observed in the KPO_3-rich corner at low concentrations of other components (up to 25 and 40 mol% of K_2WO_4 and $K_2W_2O_7$, respectively). It is worth noticing that melts, corresponding to this area have pronounced trend to over-cooling. The crystallization was initiated by mixing with platinum stirrer at 860–880 K. Stirring of

melts during slow cooling is essentially important to start nucleation in the solution, in case of not mixing only glass can be obtained. The DTA data revealed complex thermal behavior of $K_{6.5}Bi_{2.5}W_4P_6O_{34}$: endothermic effect at 840–900 K, which can be assigned to phase transition, and at 1009 K corresponding to melting.

The widest region in the central part of the diagram corresponds to $K_2Bi(PO_4)(WO_4)$ formation at the initial percentage of K_2WO_4 lower than 75 mol% and content of the other components limited by 12–55 mol%. In contrast to previous compound plate-shaped crystals of $K_2Bi(PO_4)(WO_4)$ were easily obtained without stirring at 1010–950 K. The DTA curve indicates thermal stability without phase transitions up to melting point 1013 K. Increasing of the $K_2W_2O_7$ quantity in the initial melts leads to cocrystallization of latter compound and Bi_2WO_6 (ranges of K_2WO_4, $K_2W_2O_7$ and KPO_3 concentrations are 7–20, 65–70, 25–35 mol%, respectively). Latter area develops into the second biphasic field, where Bi_2WO_6 and $KBi(WO_4)_2$ were found at 870–850 K with decreasing K_2WO_4 content down to 0–5 mol%. This region adheres to KPO_3–$K_2W_2O_7$ side of diagram, which is in agreement with precise binary phase diagram K_2O–WO_3–Bi_2O_3 [19,20] as well as the last field of Bi_2WO_6 formation in the $K_2W_2O_7$-rich corner at 830–800 K. During our investigation pure $KBi(WO_4)_2$ was not prepared due to the relatively high concentration of Bi_2O_3 that agrees well with previously reported [19]. Solutions corresponding to last two biphasic regions have pronounced disposition toward over-cooling as it was mentioned above. Consequently, this trend of formation of the crystals under mechanic effect was observed in melts at KPO_3 and $K_2W_2O_7$-rich corners, whereas at K_2WO_4 corner glass was formed even in case of intensive stirring.

Basically, the logic way of compounds crystallization can be clearly marked as follows: compounds with phosphate lattice appear in phosphate-rich area; approximately equal proportion of phosphate and tungstate components gives rise to formation of mixed phosphate–tungstate framework and prevalence of tungstate in the melt stimulates the crystallization of compounds with tungstate lattices.

3.2. Crystal structure of $K_{6.5}Bi_{2.5}W_4P_6O_{34}$

The structure of $K_{6.5}Bi_{2.5}W_4P_6O_{34}$ possesses layered architecture and consists of $\{K_7Bi_5W_8P_{12}O_{68}\}_\infty$ layers parallel to *ab* plane. These anionic layers are stacked along direction *c* and separated by sheets of potassium atoms (K1, K2, K3 and K4) (Fig. 2). Additionally, this layer shows complex sandwich-like structure. It is organized from $[BiPO_4]_\infty$ crimped network clutched by two laced $[W_2P_2O_{13}]_\infty$ layers. As a result, formed in this way $\{K_7Bi_5W_8P_{12}O_{68}\}_\infty$ layered framework is penetrated by multidirectional tunnels filled by the potassium and bismuth atoms (positions K5/Bi5, K6/Bi6, K7/Bi7 and K8/Bi8).

As it was mentioned, the simplest parts of the $\{K_7Bi_5W_8P_{12}O_{68}\}_\infty$ layer are $[W_2P_2O_{13}]_\infty$ and $[BiPO_4]_\infty$. The first one is built up from W_2O_{11} bioctahedral units linked together with PO_4 tetrahedra in vertices sharing manner (Fig. 3). Consequently, the linkage of the $[W_4P_4O_{26}]$ blocks gives rise to formation of eight-side windows, where K5 and K6 atoms are located. The architecture of this layer is topologically identical to that found in minyulite $K[Al_2F(H_2O)_4(PO_4)_2]$ [21]. In comparison with the title compound, a bioctahedral unit is built up from $[AlO_5F]_2$ dimer, where fluorine plays bridging role with Al–F–Al angle 133.3(4)°, whereas bridging angles of both W_2O_{11} in $K_{6.5}Bi_{2.5}W_4P_6O_{34}$ structure are 147,97(6) and 149,20(6)°.

The second part of $\{K_7Bi_5W_8P_{12}O_{68}\}_\infty$ layer, $[BiPO_4]$ goffered network. Connection of two types of Bi atoms with orthophosphate tetrahedra in corrugated manner is shown in Fig. 4. Both sublayers are stacked in a sandwich-like manner forming tunnels, where K7/Bi7 and K8/Bi8 atoms exist.

In comparison with $KBi(WO_4)_2$, where BiO_8 is relatively regular tetragonal antiprism, all unique bismuth polyhedra of $K_{6.5}Bi_{2.5}W_4P_6O_{34}$ structure are highly distorted (Fig. 5) due to the existence of stereoactive $6s^2$ lone pair of electrons (LPE) [22,23], which can be illustrated by corresponding values of Bi–O bond lengths. Bi1 is eight-coordinated: five the nearest Bi–O distances in range 2.19–2.70 Å form open polyhedra and three further ones with maximum bond length 3.16 Å complete the shape of $Bi(1)O_8$. Another bismuth atom has seven-fold coordination with four close distances 2.11–2.30 Å and three distant ones in range

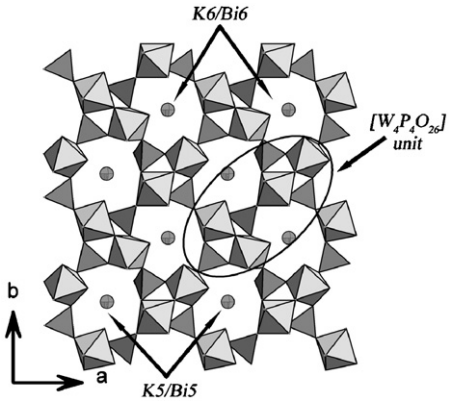

Fig. 3. View of $[W_2P_2O_{13}]_\infty$ network parallel to *ab* plane and location of potassium atoms inside eight-sided windows.

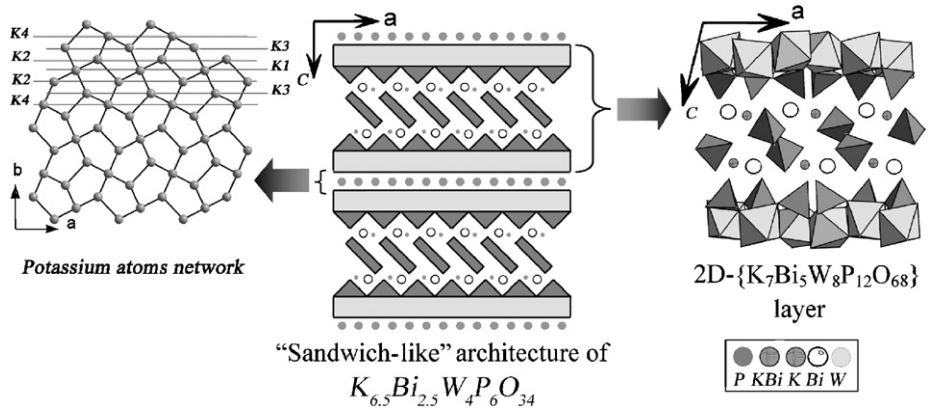

Fig. 2. Sandwich-like architecture of $K_{6.5}Bi_{2.5}W_4P_6O_{34}$. Organization of $\{K_7Bi_5W_8P_{12}O_{68}\}_\infty$ and potassium network-like building layers.

2.83–3.21 Å. Calculated values of BVS were found to be 3.02 and 3.21 for Bi1 and Bi2, respectively (Table 3). This bond dispersion and shape irregularity is quite common for bismuth polyhedra in rigid phosphate framework. Taking into account this peculiarity there were proposed two main approaches of description: consideration of open polyhedron with highlighted LPE stereoactivity, for example, pyramidal BiO_2 chains [24] and highly distorted completed polyhedron with widened spread of bond distances. For instance, eight-fold coordination of Bi with cut-off distance 3 Å is described for $Bi_{6.67}O_4(PO_4)_4$ [25], $M_{0.5}Bi_3P_2O_{10}$ (M = Ca, Sr, Ba, Pb) [26] and $Pb_5Bi_{18}P_4O_{42}$ [27] or even up to 3.16 Å for $Ba_3Bi_2(PO_4)_4$ [28]. Moreover, the organization of these polyhedra into chains [24], layers [11] and three-dimensional frameworks [29] was admitted to be very common for orthophosphate-based compounds. As a matter of fact, very few structures of bismuth orthophosphates are known to be consisting from isolated [30] or pairs of corner/edge-sharing BiO_x [31]. The title compound shows rarely observed distinct pair of corner-sharing polyhedra with the shortest Bi–Bi distance 4.87 Å.

Distortion of WO_6 octahedra, which are connected via common vertex forming W_2O_{11} bioctahedral units, is similar for all four types of WO_6 groups. Wide spread of W–O bonds in range 1.722(10)–2.184(9) Å differs slightly from earlier reported data 1.725(3)–2.196(2) Å for phosphates containing octahedrally coordinated tungsten (VI) [9,32] and indicates significant shift of tungsten atoms from the polyhedra centers. The calculated BVS values for corresponding W atoms are in range of 5.95–6.25 Å, which are close to chemical valences. More distorted WO_6 octahedra are observed for $KBi(WO_4)_2$ structure containing double ribbons of vertex-sharing $(WO_6)_2$ with wider spread of W–O bonds 1.72–2.32 Å due to more complicated octahedral organization.

Six types of orthophosphate tetrahedra were found to exist in the structure. They all are asymmetrically distorted with P–O bond lengths limited by 1.47–1.58 Å (Table 3). The corresponding values of BVS vary from 4.83 to 5.35. The observed deviation of BVS of these atoms in rigid environment from their chemical valences proves high polyhedral distortion, and strain of framework overall.

Coordination numbers of potassium atoms located in the interlayered space vary from eight to eleven. The corresponding polyhedra of potassium environments are following: $K1O_8$ is slightly distorted cube, $K4O_8$ and $K2O_{10}$ are tetragonal and pentagonal prisms, respectively, and, finally, $K3O_{11}$ is one-capped pentagonal prism (Fig. 5). Potassium atoms in K5/Bi5 and K6/Bi6 positions are 10-coordinated. These sites are partially occupied by bismuth with corresponding occupancies equal to 0.044 and 0.056. Concurrent filling of cations' positions by potassium and bismuth is also observed for K7/Bi7 and K8/Bi8 sites. Fractions of bismuth in latter positions are significantly higher than in K5/Bi5 and K6/Bi6, and equal to 0.075 and 0.325. Both positions have open polyhedra (Fig. 5). The BVS values of the potassium located between anionic layers are close to 1, BVS of K5 and K6 also is close to 1, in contrast, the BVS of K7 and K8 atoms with open

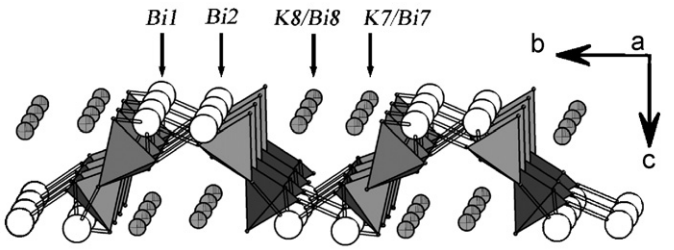

Fig. 4. Formation of [$BiPO_4$] goffered network and sites K7/Bi7 and K8/Bi8.

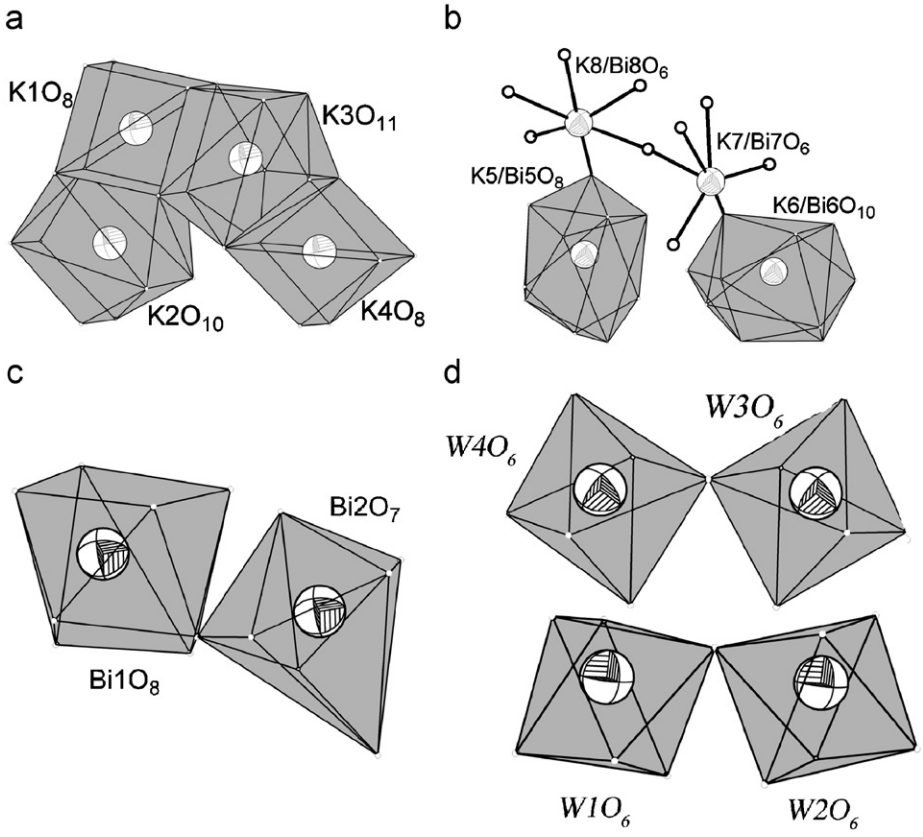

Fig. 5. Coordination polyhedra of potassium, bismuth and tungsten atoms in $K_{6.5}Bi_{2.5}W_4P_6O_{34}$.

polyhedra significantly lower ~0.7. A great number of closely situated positions of potassium (distance K–K 3.54 Å and more) inside multidirectional tunnels predict the possibility of the ionic transport and the ionic conductivity of the reported compound.

Bond-valence calculations were performed taking into account the parameters reported by Brown and Altermatt [33] for all types of atoms except potassium, while for latter element the parameters were taken from those reported by Adams [34]. The sum of BVS of positively charged phosphorus and metal atoms per $K_{6.5}Bi_{2.5}W_4P_6O_{34}$ formula unit including their occupancies were found to be 67.88, while the sum of all oxygen atoms is equal to −68.

Description of $KBi(WO_4)_2$ [19] and $K_2Bi(PO_4)(WO_4)$ [11] structures was reported earlier and is omitted herein.

3.3. FTIR-spectroscopy

$K_2Bi(PO_4)(WO_4)$ (I) and $K_{6.5}Bi_{2.5}W_4P_6O_{34}$ (II) containing PO_4 group simultaneously with WO_n polyhedra were comparatively characterized by the FTIR-spectroscopy (Fig. 6).

From spectroscopic point of view structure (I) can be considered as built up from WO_4^{2-}, PO_4^{3-} groups and K^+, Bi^{3+} cations. According to factor group analysis *Ibca* space group possesses D_{2h} factor group, which consists of A_g, B_g (Raman active) and A_u, B_u (IR-active) internal vibration modes. They could be subdivided into $A_g+A_u+2B_{1g}+2B_{1u}+2B_{2g}+2B_{2u}+B_{3g}+B_{3u}$ translation motions for each tetrahedron.

Free WO_4^{2-} and PO_4^{3-} ions, having T_d symmetry, should exhibit the presence of $\nu_1(A_1)$ and $\nu_3(F_2)$ stretching and $\nu_2(E)$, $\nu_4(F_2)$ bending modes. Among them, only ν_3 and ν_4 are IR-active and should split into triplet for each unique tetrahedron. Both tetrahedra in (I) having local symmetry C_{2v} exhibit all the bands predicted by group theory. Thus, two highest frequency bands observed in the 1055–940 region (1055 s and 946 s cm^{-1}) were assigned as asymmetric $\nu_3(F_2)$ of phosphate and symmetric $\nu_1(A_1)$ of tungstate group, respectively. Set of strong and medium bands in the area 857–748 cm^{-1} could be attributed to lattice vibrations and asymmetric stretching vibrations of WO_4. Three bands located in the lower frequency region 592–522 cm^{-1} correspond to bending modes of phosphate group.

More complicated spectrum is observed for $K_{6.5}Bi_{2.5}W_4P_6O_{34}$ due to a triclinic symmetry ($P\bar{1}$ space group). The lattice is combined from $W_2O_{11}^{10-}$, PO_4^{3-} groups and K^+, Bi^{3+} ions. Factor group analysis specifies $C_i(-1)$ factor group and corresponding A_g (Raman) and A_u (IR-active) vibration modes, which can be subdivided into $12A_g+12A_u$ translation motions of WO_6 octahedra and $18A_g+18A_u$ ones of PO_4. Starting from WO_6 octahedron with O_h symmetry, three stretching $\nu_1(A_{1g})$, $\nu_2(E_g)$, $\nu_3(F_{1u})$ and $\nu_4(F_{1u})$, $\nu_5(F_{2g})$, $\nu_6(F_{2u})$ bending modes have to be selected [35]. Only ν_3 and ν_4 are IR-active and should split into three components. In our case, resulting spectrum is much more complicated due to C_1 local symmetry and W–O–W bridge giving W_2O_{11} unit.

The spectrum of (II) consists of two separated regions: 1185–878 and 752–412 cm^{-1}. First one corresponds to the asymmetric stretching modes $\nu_3(F_2)$ of six nonequivalent PO_4 groups (1185–930 cm^{-1}) and symmetric stretching mode of tungsten octahedra (878 cm^{-1}). It should be noticed, that for (II) a shift of the stretching modes of tungsten oxygen polyhedra towards lower frequencies can be observed in comparison with stretching modes of the (I). This fact can be explained by rising of coordination number of W(VI), that causes weaker interaction between WO_6 octahedra and Bi^{3+} ions and decreasing of covalent character of the W–O bonds. The second region contains one strong band belonging to $\nu_3(F_{1u})$ of WO_6 and number of medium and weak bands corresponding to superposition of bending modes of PO_4, WO_6 and lattice vibrations in the region 630–412 cm^{-1}.

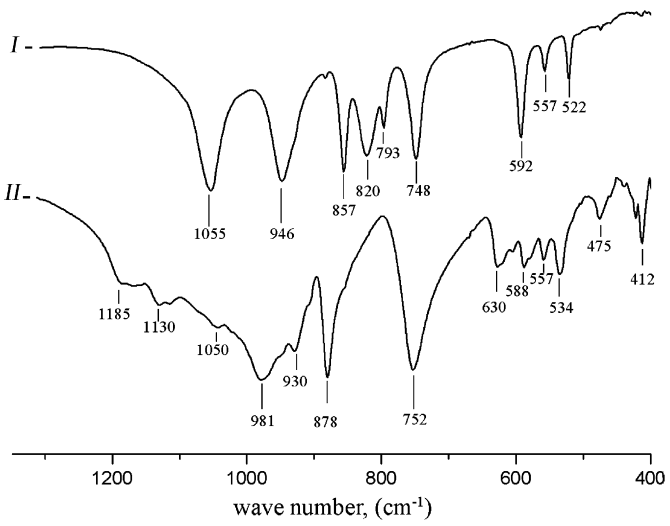

Fig. 6. FTIR-spectra of $K_2Bi(PO_4)(WO_4)$ (I) and $K_{6.5}Bi_{2.5}W_4P_6O_{34}$ (II).

4. Conclusion

Complex investigation of section $K_2W_2O_7$–K_2WO_4–KPO_3 containing 15 mol% Bi_2O_3 as a particular case of K–Bi–P–W–O system was performed by building composition diagram with crystallization fields indicated on it. Three pure compounds' regions of $K_{6.5}Bi_{2.5}W_4P_6O_{34}$, $K_2Bi(PO_4)(WO_4)$, Bi_2WO_6 and two biphasic ones were identified. Additionally, $KBi(WO_4)_2$ was obtained in a mixture with Bi_2WO_6.

$K_{6.5}Bi_{2.5}W_4P_6O_{34}$ prepared for the first time represents unusual layered architecture. The main $\{K_7Bi_5W_8P_{12}O_{68}\}_\infty$ units are separated by potassium atoms network. A great number of closely situated potassium atoms inside multidirectional tunnels predict the possibility of the ionic transport and ionic conductivity of this compound.

Acknowledgment

The authors acknowledge the ICDD for financial support (Grant #03-02).

References

[1] L. Koseva, V. Nikolov, P. Peshev, J. Alloys Compds. 353 (2003) L1–L4.
[2] M. Maczka, B. Macalik, J. Hanuza, E. Bukowska, J. Non-Cryst. Solids 352 (2006) 5586–5593.
[3] G. Poirier, Y. Messaddeq, S.J.L. Ribeiro, M. Poulain, J. Solid State Chem. 178 (2005) 1533–1538.
[4] K. Iliev, P. Peshev, V. Nikolov, I. Koseva, J. Cryst. Growth 100 (1990) 225–232.
[5] A. Grandin, A. Leclair, M.M. Borel, B. Raveau, J. Solid State Chem. 115 (1995) 521–524.
[6] D. Bravo, F.J. López, X. Ruiz, F. Díaz, Phys. Rev. B 52 (1995) 3159–3169.
[7] D.P. Shumov, M.P. Tarassov, V.S. Nikolov, J. Cryst. Growth 129 (1993) 635–639.
[8] U. Peuchert, L. Bonaty, J. Schreuer, Acta Crystallogr. C 53 (1997) 11–14.
[9] U. Peuchert, L. Bonaty, Acta Crystallogr. C 51 (1995) 1719–1721.
[10] J.S.O. Evans, T.A. Mary, A.W. Sleight, J. Solid State Chem. 120 (1995) 101–104.
[11] I.V. Zatovsky, K.V. Terebilenko, N.S. Slobodyanik, V.N. Baumer, O.V. Shishkin, Acta Crystallogr. E 62 (2006) i193–i195.
[12] B. Hamdi, H. El Feki, A.B. Salah, P. Salles, P. Baules, J.M. Savariault, Solid State Ionics 177 (2006) 1413–1420.
[13] B. Muktha, T.N. Guru Row, Inorg. Chem. 45 (2006) 4706–4711.
[14] L.A. Winger, R.C. Bradt, J.H. Hoke, J. Am. Ceram. Soc. 63 (5–6) (1980) 291–294.

[15] R. Balda, J. Fernández, I. Iparraguirre, M. Al-Saleh, Opt. Mater. 28 (2006) 1247–1252.
[16] A.A. Kaminskii, J. Garcia-Sole, D. Jaque, R. Uecker, D. Schultze, Phys. Status Solidi A 175 (1999) R9–R10.
[17] G.M. Sheldrick, SHELXS-97, University of Göttingen, Germany, 1997.
[18] G.M. Sheldrick, SHELXL-97: Program for Crystal Structure Refinement, University of Göttingen, Germany, 1997.
[19] H.D. Xie, D.Z. Shen, X.Q. Wang, G.Q. Shen, Cryst. Res. Technol. 41 (2006) 961–966.
[20] V.K. Yanovskii, V.I. Voronkova, Phys. Status Solidi A 93 (1986) 57–66.
[21] A.R. Kampf, Am. Mineral. 62 (1977) 256–262.
[22] F.A. Cotton, G. Wilkinson, Advanced Inorganic Chemistry. A Comprehensive Text, fourth ed., Wiley, New York, 2004, p. 441.
[23] H. Fujimoto, T. Yamasaki, I. Hataue, N. Koga, J. Phys. Chem. 89 (1985) 779–782.
[24] A. Mizrahi, J.-P. Wignacourt, H. Steinfink, J. Solid State Chem. 133 (1997) 516–521.
[25] S. Giraud, M. Drache, P. Conflant, J.P. Wignacourt, H. Steinfink, J. Solid State Chem. 154 (2000) 435–443.
[26] D.G. Porob, T.N. Guru Row, Acta Crystallogr. B 59 (2003) 606–610.
[27] S. Giraud, J.-P. Wignacourt, S. Swinnea, H. Steinfink, R. Harlow, J. Solid State Chem. 151 (2000) 181–189.
[28] R. Masse, A. Durif, Acta Crystallogr. C 41 (1985) 1717–1718.
[29] E. Hassan Arbib, J.P. Chminade, J. Darriet, B. Elouadi, Solid State Sci. 2 (2000) 243–247.
[30] S. Oyetola, A. Verbaere, D. Guyomard, Y. Piffard, J. Solid State Chem. 77 (1988) 102–111.
[31] X. Xun, S. Uma, A.W. Sleight, J. Alloys Compds. 338 (2002) 51–53.
[32] M. Maczka, A. Waskowska, J. Hanuza, J. Solid State Chem. 179 (2006) 103–110.
[33] I.D. Brown, D. Altermatt, Acta Crystallogr. B 41 (1985) 244–247.
[34] A. Adams, Acta Crystallogr. B 57 (2001) 278–287.
[35] K. Nakamoto, Infrared and Raman Spectra of Inorganic and Coordination Compounds, fourth ed., Wiley, New York, 1986.